View metadata, citation and similar papers at core.ac.uk
brought to you by CORE
provided by Publikationsserver der RWTH Aachen University

5th European Thermal-Sciences Conference, The Netherlands, 2008

Thermo diffusive instability phenomena of stoichiometric up to very rich spherical flames of n-heptane-air-mixtures

S. Jerzembeck, R. Dahms, O. Röhl, N. Peters
Institute of Technical Combustion, RWTH Aachen, Germany

Abstract

In this work spherical expanding N-Heptane-Air-Flames are investigated using a preheated pressure vessel combined with a high speed Schlieren measurement technique. Equivalance ratios of the investigated mixtures were chosen from Φ=1.0 up to Φ=3.5 and maximum mixture pressures were 20 bar. Mixtures close to the upper flammability limit were performed under microgravity conditions in the Drop Tower of Bremen University. The theory of expanding spherical flames from Matalon et al. was used for comparison with experimental results and show very good compliance with each other. Interestingly, captured flame images close to the upper flammability limits do not show any influence due to thermo diffusion instability effects, whereas in the equivalence ratio region between Φ=1.2 up to Φ=1.8 the flame is strongly influenced by instability effects.

1 Introduction

Investigations of spherically expanding flames in premixed combustible mixtures play an important role in fundamental understanding of various aspects of combustion. It can be used, for example, to determine the laminar flame speed of various combustible mixtures. When the mixture is centrally ignited, a spherical flame develops and propagates outward at a speed that asymptotes to the laminar burning velocity. Since the combustion products remain at rest as the flame expands, the burning velocity can be easily determined by measuring the rate of increase of the flame radius [1-3]. The data can also be used to determine the dependence of the burning velocity on flame stretch, and to deduce appropriate Markstein lengths for various experimental conditions. But accurate measurements of burning velocities and Markstein lengths can only be deduced from the propagation of smooth spherical flames. It is known that as the flame reaches a critical size, it becomes unstable [4,5]. The critical size and the nature of the instability (thermo diffusive or hydrodynamic) depends on the mixture composition, which affects the Lewis numbers and equivalence ratio, and on its reactivity, which includes the heat release and activation energy of the chemical reaction. Beyond criticality, the flame surface is instantaneously covered with a large number of cells and the propagation speed increases in time, so that the laminar burning velocity and Markstein length can no longer be deduced systematically from the experimental observations. There has been a large number of theoretical and experimental [2,4-7] investigations concerned with the onset of instability and the development of wrinkles on the surface of nominally spherical flames.

Gaseous fuels like hydrogen and methane have been widely investigated experimentally. These studies have focused on the determination of the laminar burning velocity and the onset of instabilities for pressures of up to 60 bar and equivalence ratios ranging between the flammability limits [2,6,8]. Despite their practical importance, experimental data for combustible mixtures that contain liquid fuels at ambient conditions, for example n-heptane and iso-octane, are rather scarce. And for very rich mixtures, especially close to the upper flammability limit, no experimental data can be found. The objective of this paper is to fill this gap and to present results on fundamental flame properties for such fuels.

N-Heptane-Air-Mixture flames were investigated at 20 bar initial pressure and 373 K initial temperature for equivalence ratios from Φ=1.0 up to Φ=2.0 under gravity conditions. One N-

Heptane-Air-Mixture (Φ=3.5, T=420 K and p=20 bar) was investigated under microgravity conditions to avoid the influence of buoyancy forces on the expanding flame due to the slow expansion propagation velocity. Stretch effects due to buoyancy force can stabilize the propagating flame front and can avoid the development of thermo diffusion cells. Interestingly, no instability effects for this case could be observed. The expanding flame front was as smooth as the stoichiometric mixture. Mixtures with equivalence ratios between those two mixtures start to develop thermo diffusion instabilities. Interestingly, a maximum amount of thermo diffusion cells could be observed for a mixture with the equivalence ratio of Φ=1.4. For mixtures with equivalence ratios larger than Φ=1.4 the amount of developed cells decreased with mixtures becoming richer. A theory for spherical flame propagation developed by Matalon et al. was used for numerical comparison with the experimental results.

2 Theory

As the flame propagates outwards it is stretched. The stretch rate κ, defined as the relative rate of change of the flame surface area A, is given by

$$\kappa = \frac{1}{A}\frac{dA}{dt} = \frac{2}{R_b}\frac{dR_b}{dt} \qquad (1)$$

where t represents time. An explicit dependence of flame speed on stretch was obtained by Matalon et al. [9] in a general theory for a two-component mixture with temperature-dependent properties that undergoes a global one-step chemical reaction, and a detailed discussion on spherical flames appeared in [10]. The theory is based on the assumptions that the flame is thin, $l_f / R_b << 1$, and the activation energy or Zel'dovich number is large $\beta = E(T_b - T_u)/RT_b^2$; here E is the overall activation energy of the chemical reaction, R is the gas constant and T is the temperature with subscripts $_u$, $_b$ representing the state of the unburned, burned gas respectively. For a spherically expanding flame, the propagation speed is given by $dR_b / dt = \sigma s_L - \mathcal{L}_b \kappa$, where s_L is the (unburned) laminar burning velocity, $\sigma = \rho_u/\rho_b$ the density ratio of the unburned-to-burned gas, or the thermal expansion parameter, and $\mathcal{L}_b$ is the Markstein length[#]. Noting that, to leading order, $dR_b / dt \sim \sigma s_L$ this expression can be simplified to

$$dR_b / dt = \sigma s_L (1 - 2\mathcal{L}_b / R_b) \qquad (2)$$

The Markstein length $\mathcal{L}_b$ [1], which accounts for diffusion influences within the flame zone, is of the order of the flame thickness and is given by

$$\mathcal{L}_b = \frac{\sigma}{\sigma - 1}\left\{ \int_1^\sigma \frac{\lambda(x)}{x} dx + \frac{1}{2}\beta(Le_{\text{eff}} - 1) \int_1^\sigma \frac{\lambda(x)}{x} \ln\frac{\sigma - 1}{x - 1} dx \right\} l_f .$$

It depends on thermal expansion and on the effective Lewis number $Le_{\text{eff}} = (Le_F + \mathcal{A} Le_O)/(1 + \mathcal{A})$ of the mixture, where λ = λ(T) is the thermal conductivity of the mixture, Le_F and Le_O are the individual Lewis Numbers of the fuel and oxidizer and $\mathcal{A} = 1 + \beta(\phi - 1)$ measures the departure from stoichiometry with $\phi = (Y_{Fu}/\nu_F W_F)/(Y_{Ou}/\nu_O W_O)$ the equivalence ratio and ν_i, W_i, Y_i the

stoichiometric coefficient, molecular weight and mass fraction of species *i*. We note parenthetically that the expression for $\mathcal{A}$ is only valid for rich mixtures; for lean mixtures ϕ must be replaced by ϕ^{-1}; these details and the generalization of $\mathcal{A}$ to arbitrary reaction orders can be found in the referenced papers.

Since the burned gas for an outward-propagating flame is motionless, the recorded flame front displacement dR_b/dt corresponds to the (burned) laminar burning velocity. In Figure 3 we show a comparison of the image-processed flame results of the experiments and the predictions of the hydrodynamical flame model. The graphs compare the dependence of the propagation speed on flame radius (equivalent to time) and its dependence on stretch for N-Heptane- and Iso-octane/Air mixtures. The symbols in this figure correspond to the experimental data while the solid curves are obtained from the theoretical formulas. Before discussing the results we comment on how the parameters appearing in these expressions were determined. Density ratios, or thermal expansion parameters, were computed with the one dimensional flame code CANTERA [11] and the described mechanism for n-heptane and iso-octane [7]. The activation energy appearing in the Zel'dovich number was calculated using the formula by Peters and Williams [12], namely

$$\frac{E}{R} = -2\frac{d(\rho_u s_L)}{d(1/T_b)}$$

with the mass flow rate $\rho_u s_L$ obtained from a one dimensional flame calculation, and the adiabatic flame temperature from a homogeneous reactor calculation at constant pressure and enthalpy conditions. The effective Lewis number was calculated using Le_F and Le_O obtained from thermodynamical and transport data of the used skeletal mechanism. This data was also used to evaluate the thermal diffusivity D_{th} and hence the diffusion length $l_f = D_{th}/s_L$. The dependence of thermal conductivity on temperature was assumed to obey $\lambda \sim T^{1/2}$. The numerical calculated properties are summarized in table 1.

Mixtures	Le_{eff} [-]	l_d [-]	σ [-]	s_l [cm/s]	E [kJ/mol]
N-Heptane $[O_2]/([O_2]+[N_2])$ = 0.205					
Φ=1.0 (T=373K)	1.30	0.031	6.32	32.65	65
Φ=1.2 (T=373K)	1.11	0.029	6.02	32.25	62
Φ=1.4 (T=373K)	0.94	0.047	5.59	18.83	60
Φ=1.8 (T=373K)	0.82	0.108	4.83	7.64	58
Φ=2.0 (T=373K)	0.73	0.136	4.48	5.93	57
Φ=3.5 (T=420K)	0.59	0.188	3.76	3.54	71

Table 1: Numerical flame properties used in the theoretical model

3 Experiments

A detailed description of the experimental apparatus used for the present study is given in an earlier paper by Jerzembeck and Peters [14]. For clarity, the main features of the equipment and the procedures used to carry out the measurements will be described here. Figure 1 illustrates the apparatus that was used for all the reported experiments. The pressurized vessel used in the present work has an inner diameter of 100 mm and offers optical access by two 50 mm diameter circular windows positioned in opposite directions. The combustible mixture is ignited in the centre of the vessel with a modified standard ignition plug with extended electrodes and a two step ignition system. The optical flame investigation was assumed to be at constant pressure, because only the early stage of spherical flame development was observed where the volume of the burnt gases is small compared to the volume of the vessel. A HeNe-Laser was used as a light source. Furthermore,

a shock resistant high-speed camera with 225 fps and a resolution of 250 x 250 pixels was used to track the spherical flame under microgravity conditions. A high-speed CCD camera with 5050 fps and a resolution of 100 x 100 pixels was used to track the spherical flame under gravity conditions. The vessel hull was heated up to approximately 543 K for enabling full evaporation of the selected fuels. The vessel was evacuated before it was filled with the combustible mixture. The necessary amount of liquid fuel was filled in through a lock system. Afterwards, the necessary amount of oxygen and nitrogen was filled in very slowly through a fine needle valve. Small heating fans inside the chamber were used for stirring the mixture. These fans were turned off approximately 5 minutes before sparking the combustible mixture.
In order to eliminate buoyancy effects, which would significantly distort the flame from its spherical shape, the experiments were performed in a microgravity environment at the Drop Tower in Bremen. The gravitational force (per unit mass) on the expanding flame was 10^{-6} g, which is significantly lower than the 10^{-2} g gravitational force that prevails in the microgravity conditions of a parabolic flight experiment.

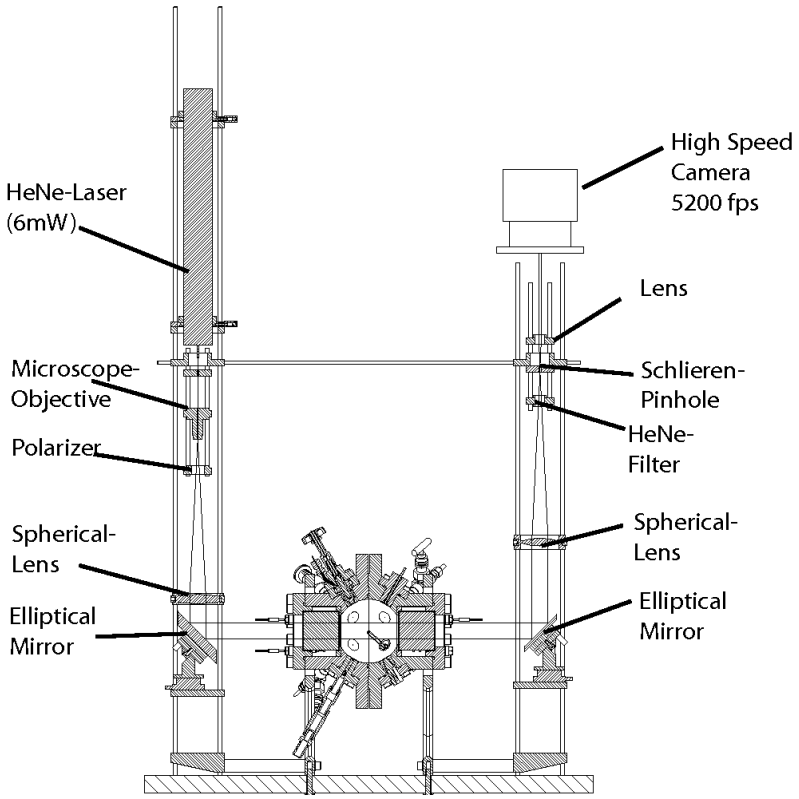

Figure 1:Experimental setup

3 Results

Figure 2 shows the flame evolution of captured spherical flame photographs of n-heptane-air-mixtures with equivalence ratios from ϕ =1.0 up to ϕ =3.5, because of the very dark background the captured flame photographs were manually adjusted by increasing the grey scale gradients, providing a better visibility of the travelling fronts. Therefore, the intensity of the photographs presented in the figure is not the same as for the truly captured photographs. Bright spots, which could hardly be seen in the original photographs, appear inside the flame (in the burned gas) of the microgravity investigated mixture. The stochiometric and the very rich flames investigated and presented in the present work appear to be smooth and nearly spherical. For flames with equivalence ratios between ϕ =1.2 up to ϕ =2.0 the development of cellular structures due to thermo

diffusion instabilities could be observed. The amount of developed cellular structures increased with increasing the equivalence ratio of the mixture up ϕ =1.4. For mixtures with equivalence ratios larger than ϕ =1.4 the development of thermo diffusion cells decreased. At equivalence ratio ϕ =2.0 the flame lifted up due to the influence of buoyancy force, but the flame front surface did not develop much cellular structures. For the very rich mixtures the flame front surface developed smooth.

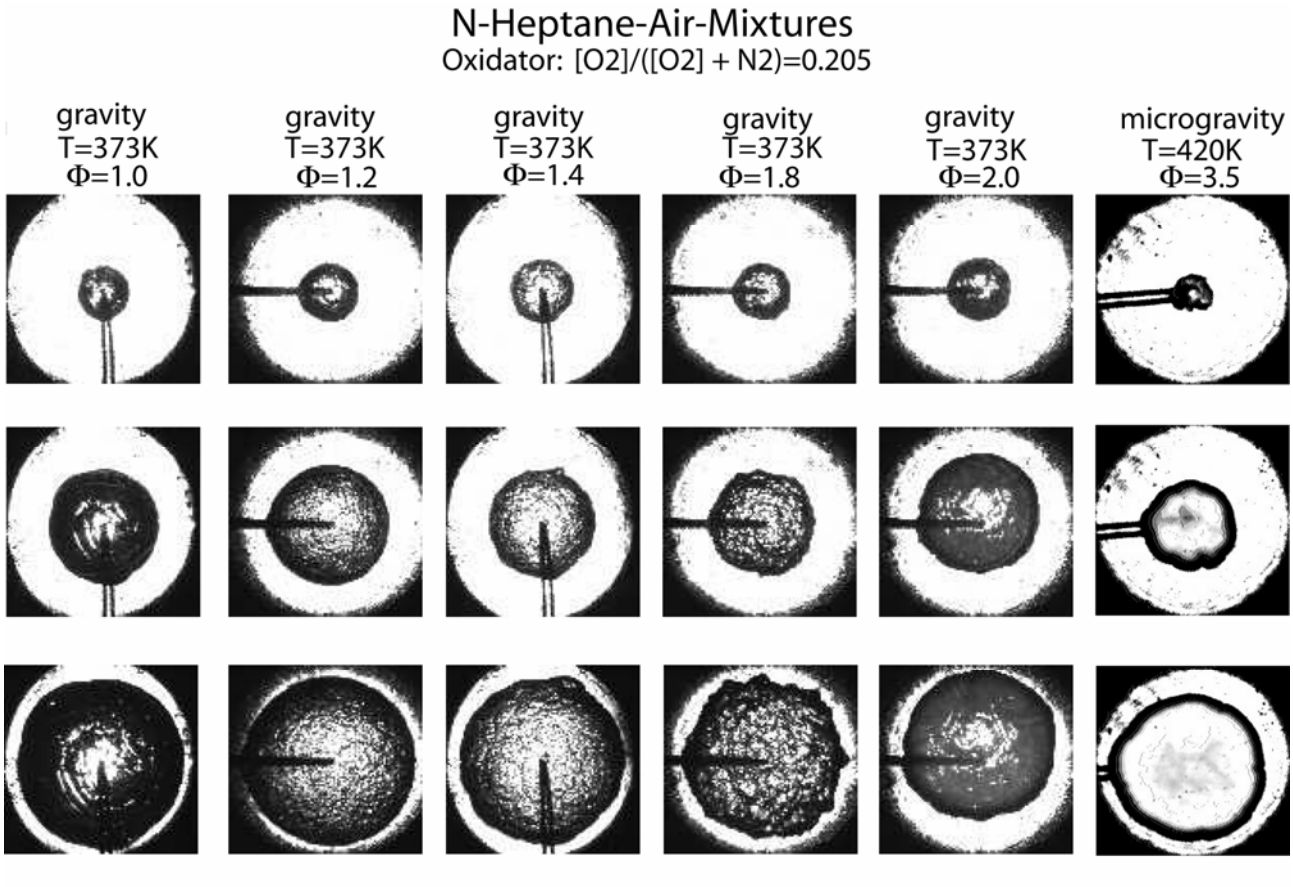

Figure 2: Tracked Schlieren-Photographs of expanding spherical flames

Figure 3 and *Figure 4* depict experimental and numerical results of the investigated spherical expanding flames. The theory of Matalon et al. was used for the comparison with the measured results. The graphs on the left hand side of Figure 3 and Figure 4 show the dependence of the propagation speed dR_b/dt on flame position R_b and the graphs on the right hand side show the corresponding propagation speed against the stretch rate κ. In accord with the theory, the tendency of the propagation speed is to decrease monotonically as R_b increases reaching the laminar burning velocity at large radii when the stretch rate $\kappa \sim 2\sigma s_L / R_b \to 0$. This in contrast to lean hydrocarbon mixtures, i.e. mixtures with sufficiently large Lewis number, for which the propagation speed of the expanding flames increases with increasing R_b as was experimentally observed by Strehlow [15] and deduced from equation (2). Also, in accord with the theory the dependence of the propagation speed on stretch is linear with a slope σL_b. There is, in general, a good agreement between the theoretical and experimental results except when the flame radius is small. This is partially attributed to the fact that the theoretical results, derived for $l_f / R_b << 1$, are not valid during the early development and partially due to the fact that the observed flames may be affected by the size of the ignition spark.

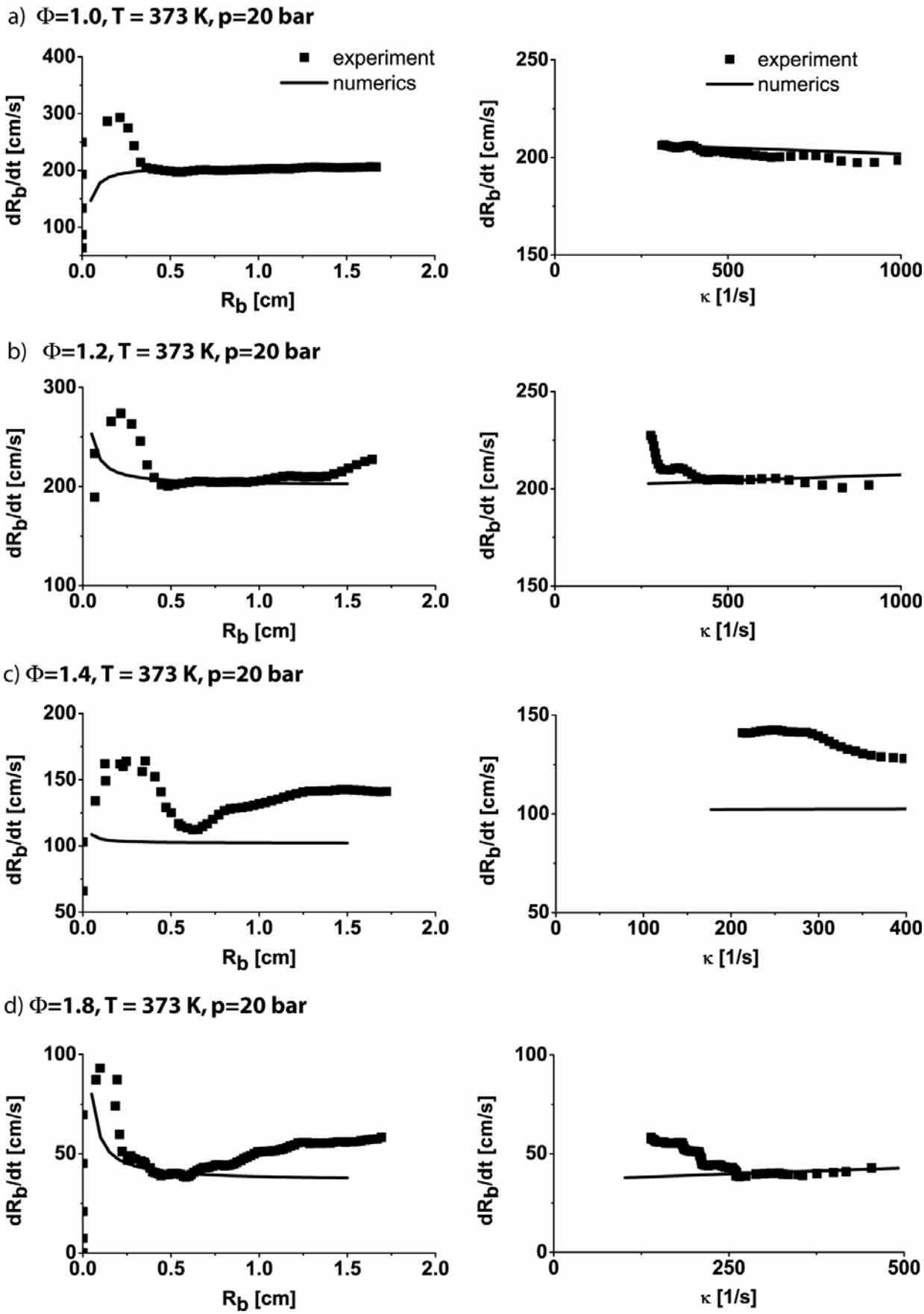

Figure 3 Comparison *between the experimental data and the theoretical predictions*

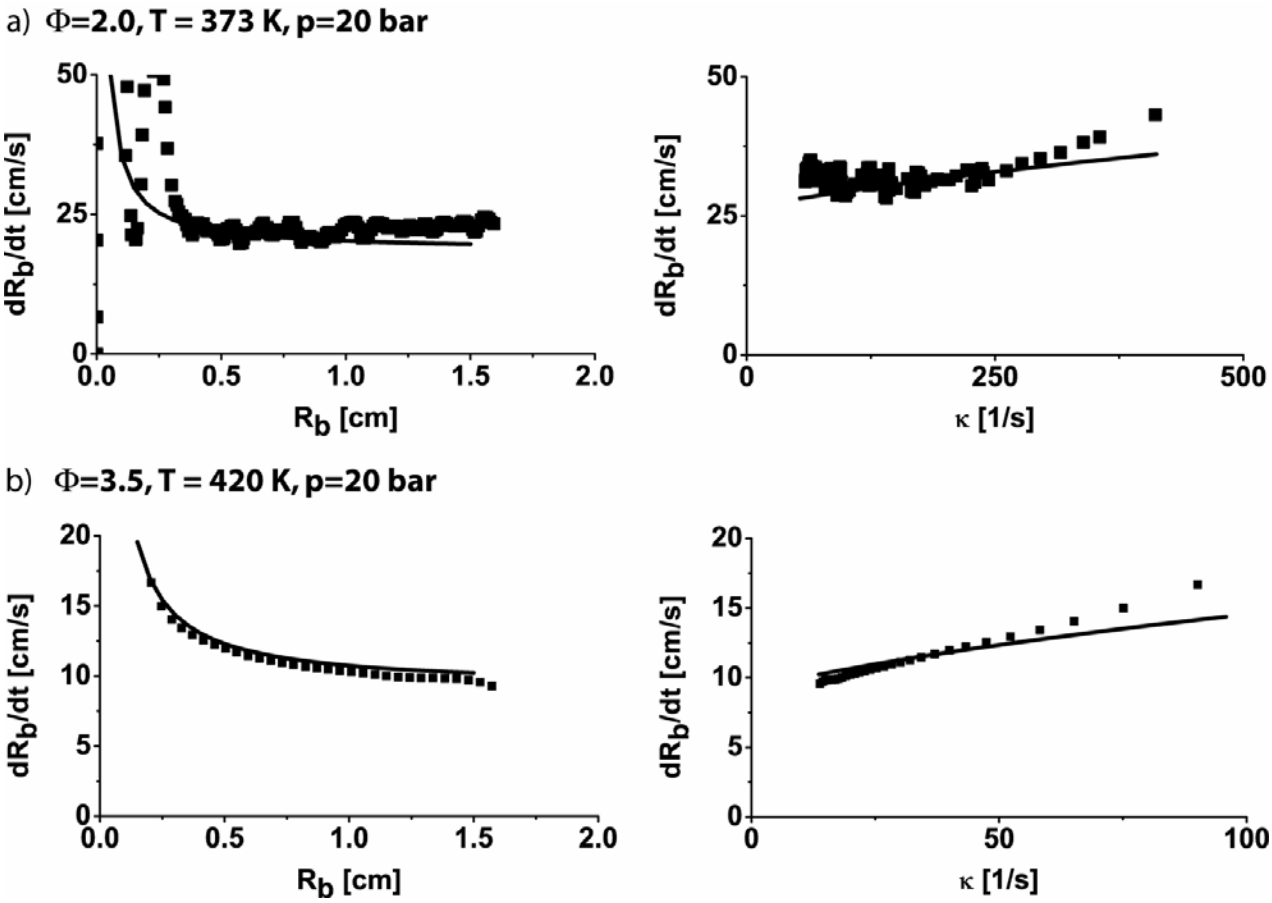

Figure 4: Comparison between the experimental data and the theoretical predictions

All experimentally investigated results apart the case ϕ =1.4 satisfy the numerical results, determined from the theory of Matalon et al. in a good way. The development of cellular structures could be observed with mixtures becoming richer. The smallest cell size due to thermo diffusion effects could be observed for the mixture with equivalence ratio ϕ =1.4. For richer mixtures the cell sizes increased and for the case ϕ =3.5 no wrinkles or cellular structures due to instability effects could be seen. This flame was smooth and satisfied the theory e.g. as good as the stoichiometric case did.

Only the experimental results of the mixture with the equivalence ratio ϕ =1.4 did not match the corresponding numerically determined ones. The experimental results were over predicted due to the massive increase in flame surface area and therefore the increase in propagation velocity. For richer mixtures with decreasing cellular structure sizes the propagation velocity decreased and a compliance with the numerically determined results were matching better as the mixture becoming richer.

It was thought that the development of cellular structures due to diffusion effects in the flame front surface become dominant when the effective Lewis-Number or the Lewis-Number of the deficient specie with respect to the unburned mixture decrease. In this work it is shown that smooth flames at stoichiometric conditions become instable due to the development of wrinkles when the mixture become rich up to an equivalence ratio of ϕ =1.4. For richer mixtures the flames started to stabilize the flame front surface with increasing the equivalence ratio of the mixture.

For further understanding of that phenomena a theory will be developed in the near future.

4 Conclusion

- Spherical expanding flames were investigated at 20 bar and 373K and 420 K for equivalence ratios between ϕ =1.0 and ϕ =3.5

-The smallest cell size development was observed for the mixture at ϕ =1.4

-The flames at stoichiometric conditions appeared to be smooth, with increasing the equivalence ratio the flames started to deveop celluar structures up to a limit of ϕ =1.4. For richer mixtures the flames were stabilized and at ϕ =3.5 the flame were smooth as well as the stoichiometric ones

- A good compliance between the experimental results and the numerical results obtained with the theory of Matalon et al. were made, apart for the case at ϕ =1.4

5 References

1. Peters N. Turbulent Combustion: University Press; 2000:320
2. Bradley D, Hicks, R.A., Lawes, R.A., Sheppard, C.G.W. and Wolley, R. The Measurement of Laminar Burning Velocities and Markstein Numbers for Iso-octane-Air and Iso-octane-n-Heptane-Air Mixtures at elevated Temperatures and Pressures in an explosion Bomb. Combustion and Flame 1998;115:126-144
3. Metgalchi M, Keck, J. C. Burning Velocities of Mixtures of Air with Methanol, Isooctane and Indolence at High Pressure and Temperature. Combustion and Flame 1982;48:191-210
4. Lockett RD. Instabilities and soot formation in spherically expanding, high pressure, rich, iso-octane-air flames. Journal of Physics: 2006;Conference Series 45:154–160
5. Kwon OC, Rozenchan, G., Law, C. K. Cellular Instabilities and Self-Acceleration of Outwardly Propagating Spherical Flames. Proceedings of the Combustion Institute 2002;29:1775-1783
6. Rozenchan G, Zhu, D.L., Law, C.K. Proceedings of the Combustion Institute 2002;29:1461-1469
7. Jerzembeck S, Peters, N., Pepiot-Desjardins, P., Pitsch, H. Laminar burning velocities at high pressure for primary reference fuels and gasolin: Experimental and numerical investigation. Combustion and Flame to be submitted
8. Bradley D, Sheppard G. W., Woolley, R., Greenhalgh, D. A., Lockett R. D. The Development and Structure of Flame Instabilities and Cellularity at Low Markstein Numbers in Explosions. Combustion and Flame 2000;122:195-209
9. Matalon M, Cui, C., Bechtold, J . Journal of Fluid Mechanics 2003;487:179-210
10. Bechtold JK, Cui, C., Matalon, M. The role of radiative losses in self-extinguishing and self-wrinkling flames. Proceedings of the Combustion Institute 2005;30:177-184
11. Goodwin D. Cantera : Object-oriented software for reacting flows, Technical report. In: , California Institute of Technology; 2005
12. Peters N, Williams, F. A. Combust Flame 1987;68:185
13. Fansler TD, Drake, M. C., Düwel, I., Zimmermann, F. P. Fuel-Spray and Spark-Plug Interactions in a Spray-Guided Direct-Injection Gasoline Engine. In, AVL Symposium; 2006
14. Jerzembeck S, Peters, N. Measurements of Laminar Flame Velocity and Markstein Length for Standard Gasoline and a Corresponding Reference Fuel Mixture (PRF87) SAE 2007
15. Strehlow RA. Fundamental of Combustion
2nd ed. NY: McGraw Hill; 1984:433
16. Otsu N. A Threshhold Selection Method from Grey Level Histogram. IEEE Transaction on Systems Managment and Cybernetics 1979;SMC-9:62-67